FiO+LS 2019 (FTu5C.5)
September 17, 16:30-16:45 2019

Dispersion Engineering of Crystalline Microresonator Fabricated with Computer-controlled Diamond Turning

Shun Fujii[1], Yuka Hayama[2], Shuya Tanaka[1], Shota Sota[1], Koshiro Wada[1], Yasuhiro Kakinuma[2], and Takasumi Tanabe[1]

1. Department of Electronics and Electrical Engineering, Faculty of Science and Technology, Keio University
2. Department of System Design Engineering, Faculty of Science and Technology, Keio University

Outline

1. Background and motivation
2. Dispersion engineering of MgF_2 microresonators
3. Fabrication by computer-controlled turning
4. Phase-matched four-wave mixing (μ-comb generation)
5. Conclusion

Ultrahigh-Q optical microresonators

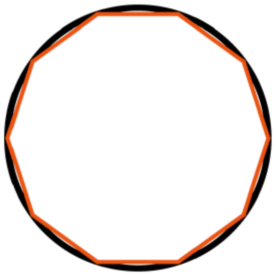

Whispering gallery mode (WGM) optical microresonator

Confines light for long photon lifetime (high Q) and has small volume

Enhances light-matter interaction in dielectric material

Dielectric microresonator platforms (Caltech, NIST, EPFL, OEwaves, Columbia, Harvard, Yale, INRS-EMT)

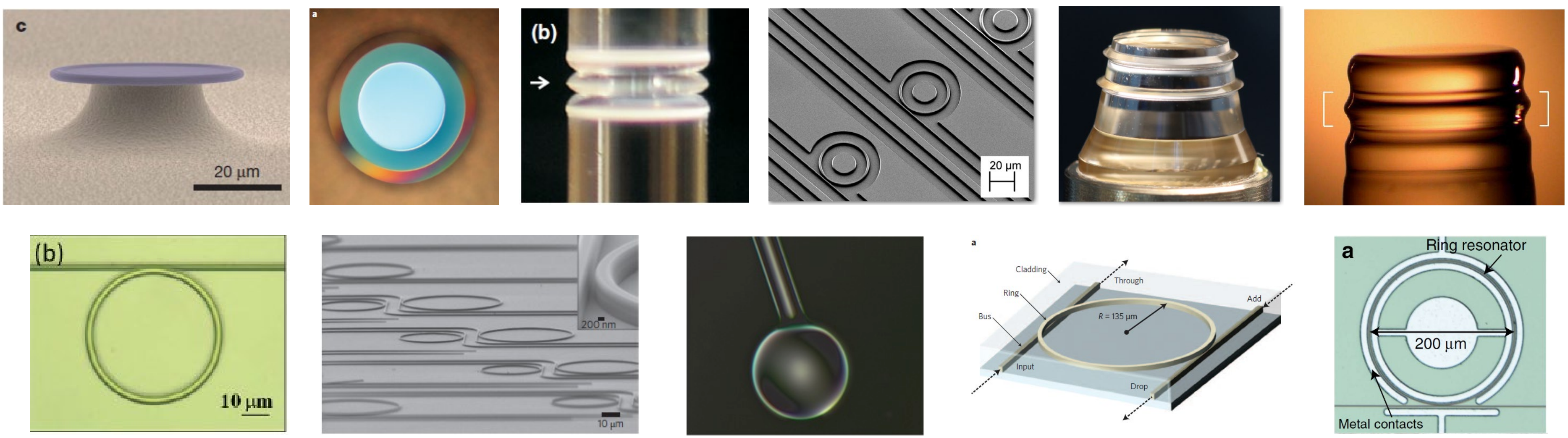

$$(\text{Intracavity power}) = \frac{4\eta d_1 Q}{\omega_0} \times (\text{Input power})$$

ω_0: laser frequency, d_1: cavity FSR,
Q: quality factor, η: coupling parameter

e.g. $\omega_0/2\pi = 193$ THz, $d_1 = 100$ GHz,
$Q = 1 \times 10^8$, $\eta = 0.5$ (critical coupling)

10 mW input ⇒ 165 W intracavity

Application: Microresonator comb

Target application: Microresonator frequency comb (Kerr comb)

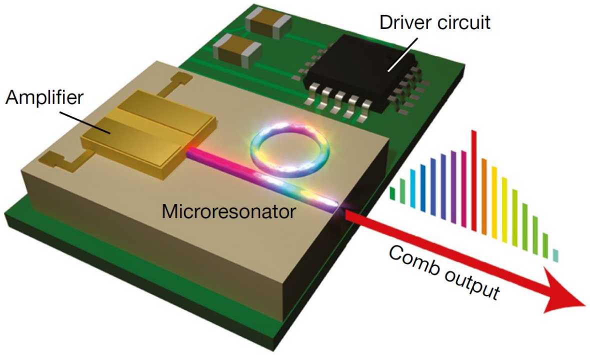

Nature 562, 401–405 (2018)

Four-wave mixing (FWM)

$$\omega_a + \omega_{b(a)} = \omega_c + \omega_d$$

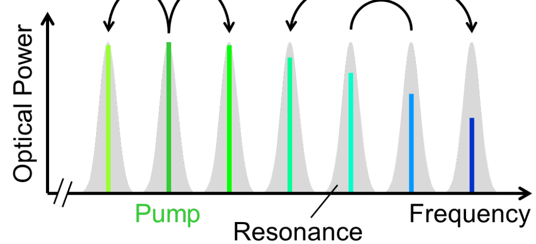

Threshold power for FWM

$$P_{th} = \frac{\kappa^2 n_0^2 V_{eff}}{8\eta\omega_0 c n_2} \propto \frac{V}{n_2 Q^2}$$

- Compact size
- Low energy consumption
- Broad bandwidth
- Large mode spacing ~1000 GHz

Microresonator dispersion and the effect on microcomb spectrum

Material dispersion

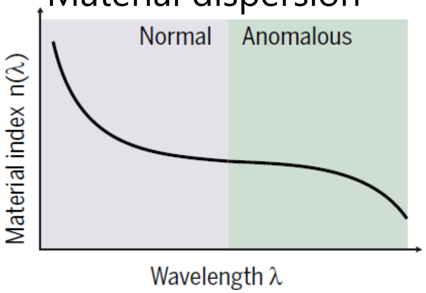

Geometrical dispersion

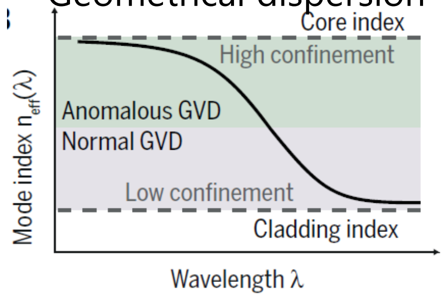

Sign and value of D_n determines optical spectrum

$$\omega_\mu = \omega_0 + D_1\mu + \frac{1}{2}D_2\mu^2 + \frac{1}{6}D_3\mu^3 + \frac{1}{24}D_4\mu^4 \cdots$$

$D_2 > 0 \;\; D_3, D_4 \sim 0$ $\quad$ $D_2 > 0 \;\; D_3 < 0, D_4 \sim 0$

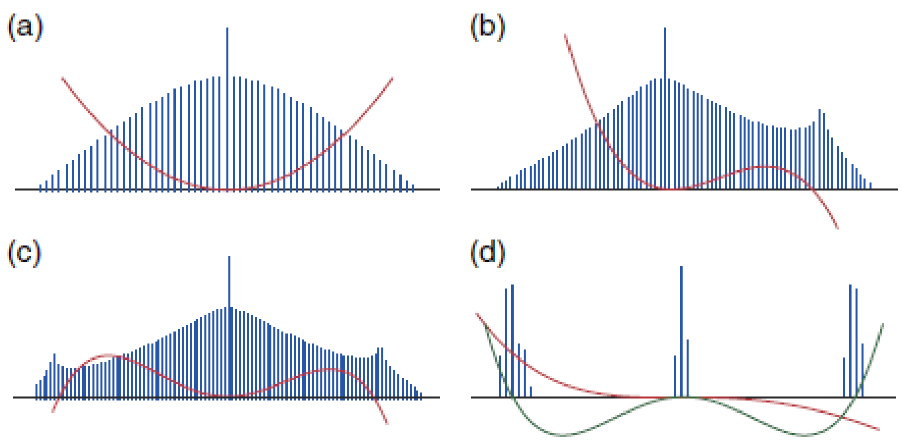

$D_2 > 0 \;\; D_3 < 0, D_4 < 0$ $\quad$ $D_2 \leq 0 \;\; D_3 < 0, D_4 > 0$

Dispersion control in high-Q resonator

GVD parameters β_2 for MgF_2 microresonators with different FSRs

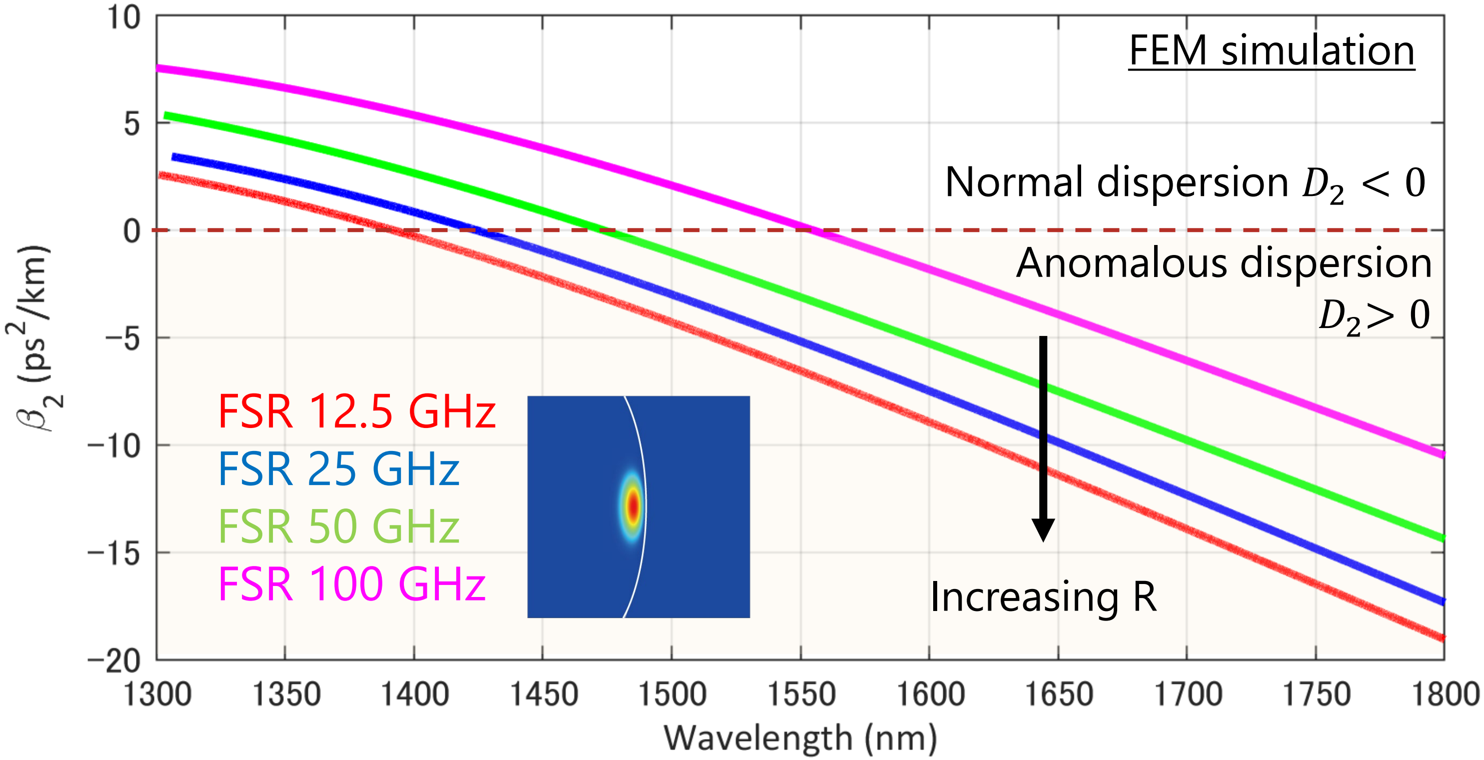

- 100 GHz FSR microresonator shows weak normal dispersion in 1550 nm band
- Geometrical dispersion limits microcomb generation in small-R MgF_2 resonator

Motivation

Fabrication method of crystalline microresonator

Hand Polishing	Fluoride crystal MgF_2 CaF_2 BaF_2 $LiNbO_3$(PPLN)	Q ~ 10^{10}	Ultra-high Q Form accuracy ✘
Machining		Q ~ 10^{8}	High-Q Form accuracy ❍

- Fabricate ultra-high Q crystalline microresonators (Q>10^8) by computer-controlled machining **without polishing process**

- Explore resonator cross-section which realizes anomalous dispersion for 100 GHz free-spectral range (FSR) crystalline microresonators

Overcome Q limitation to achieve 100 GHz FSR microcomb generation

Dispersion control in high-Q resonator

GVD parameters β_2 for "100 GHz" MgF_2 microresonators

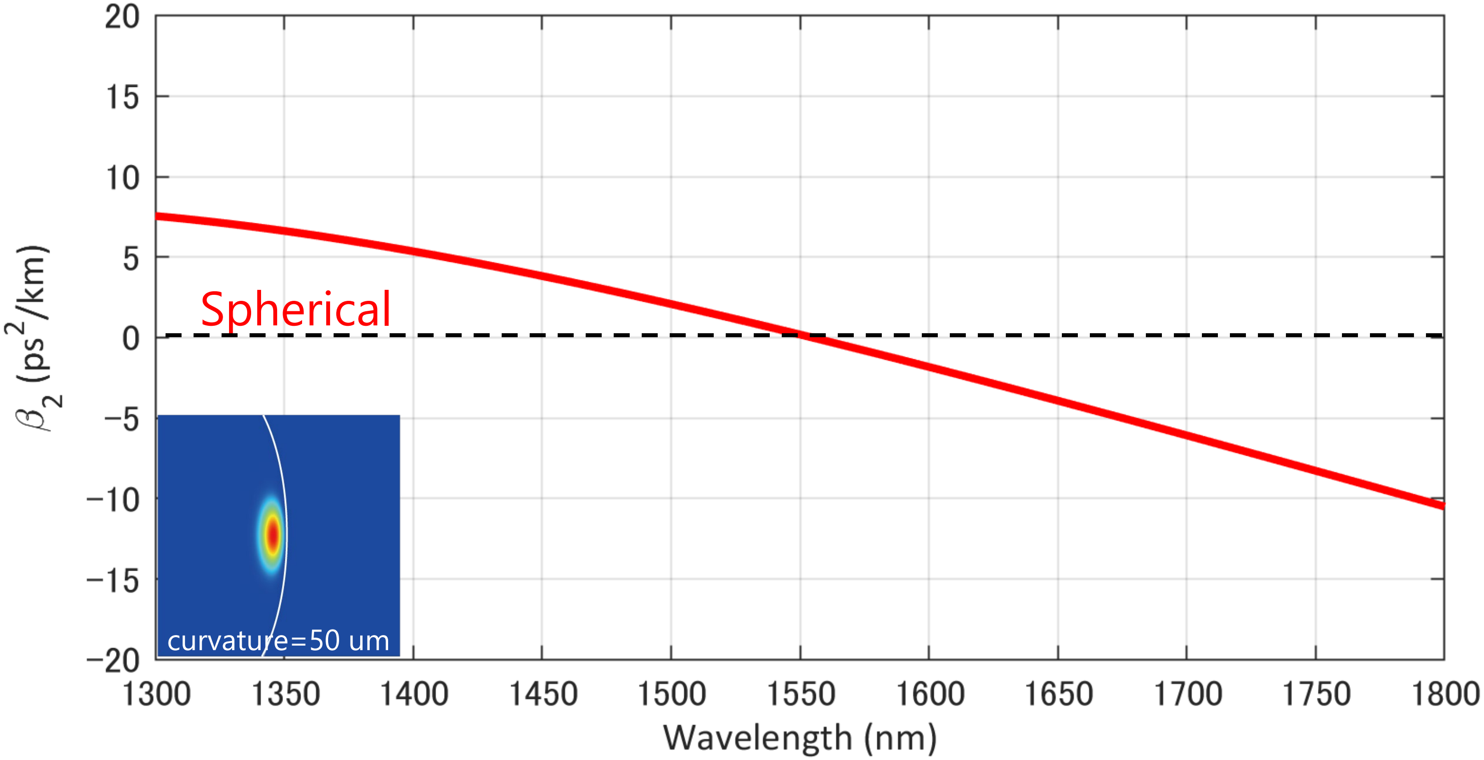

Dispersion control in high-Q resonator

GVD parameters β_2 for "100 GHz" MgF_2 microresonators

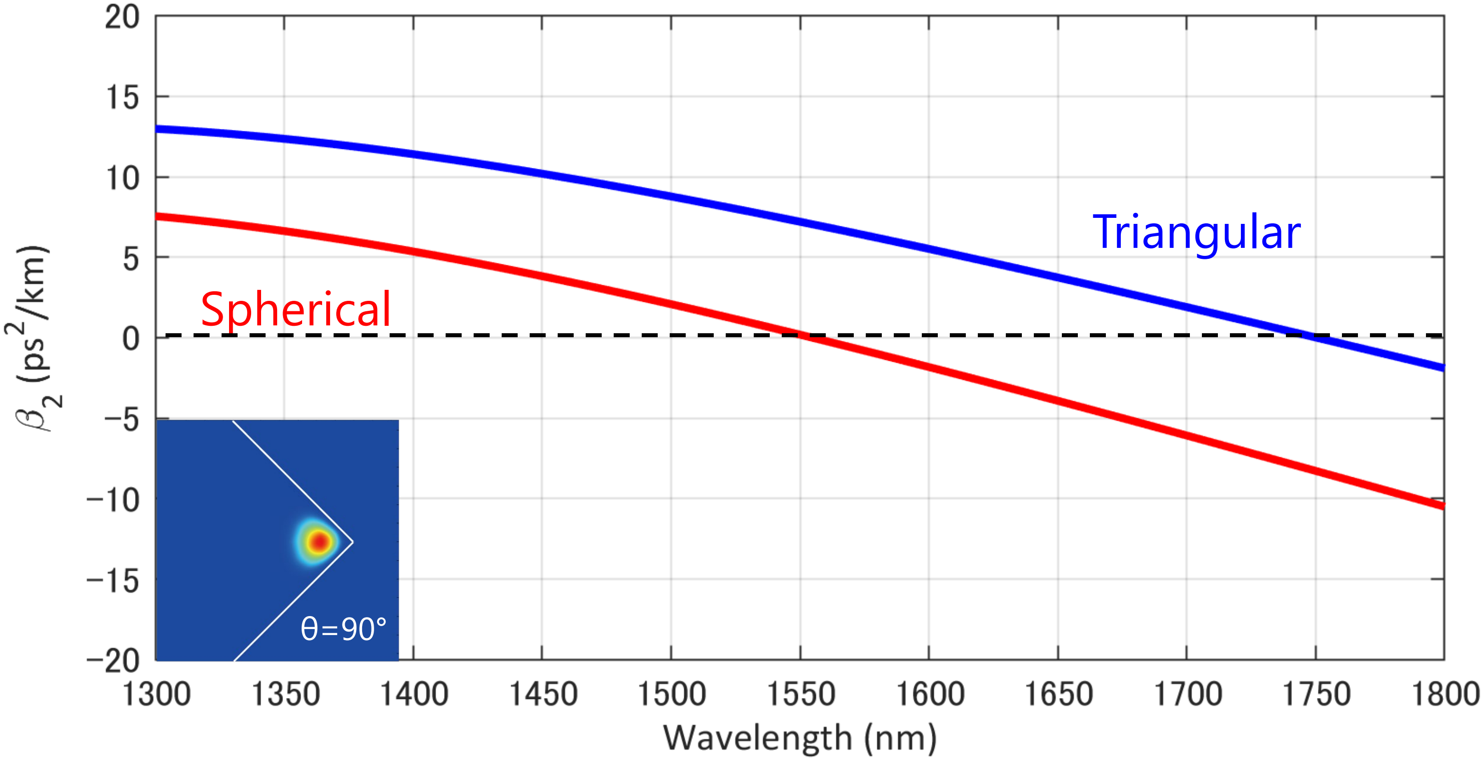

Dispersion control in high-Q resonator

GVD parameters β_2 for "100 GHz" MgF_2 microresonators

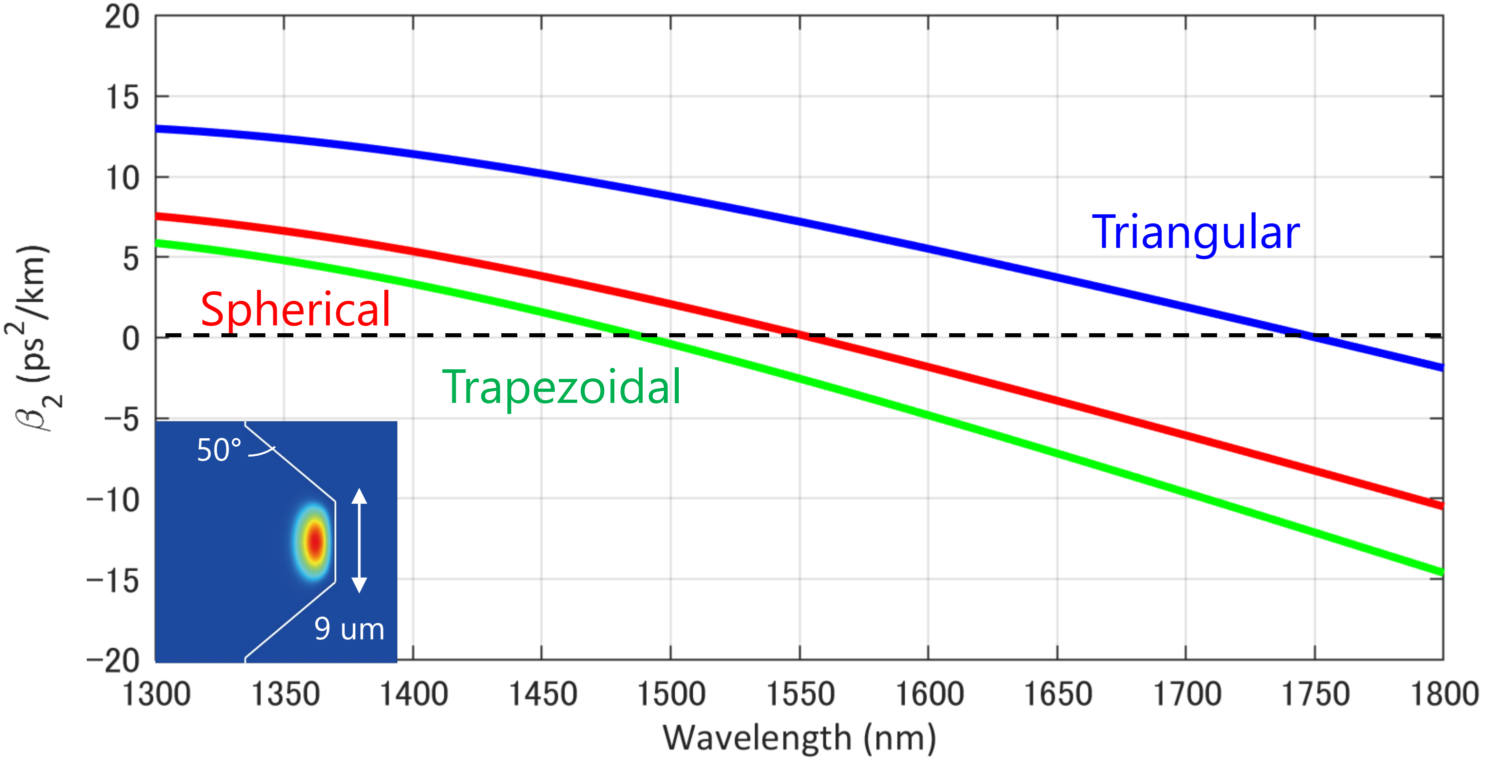

Dispersion control in high-Q resonator

GVD parameters β_2 for "100 GHz" MgF_2 microresonators

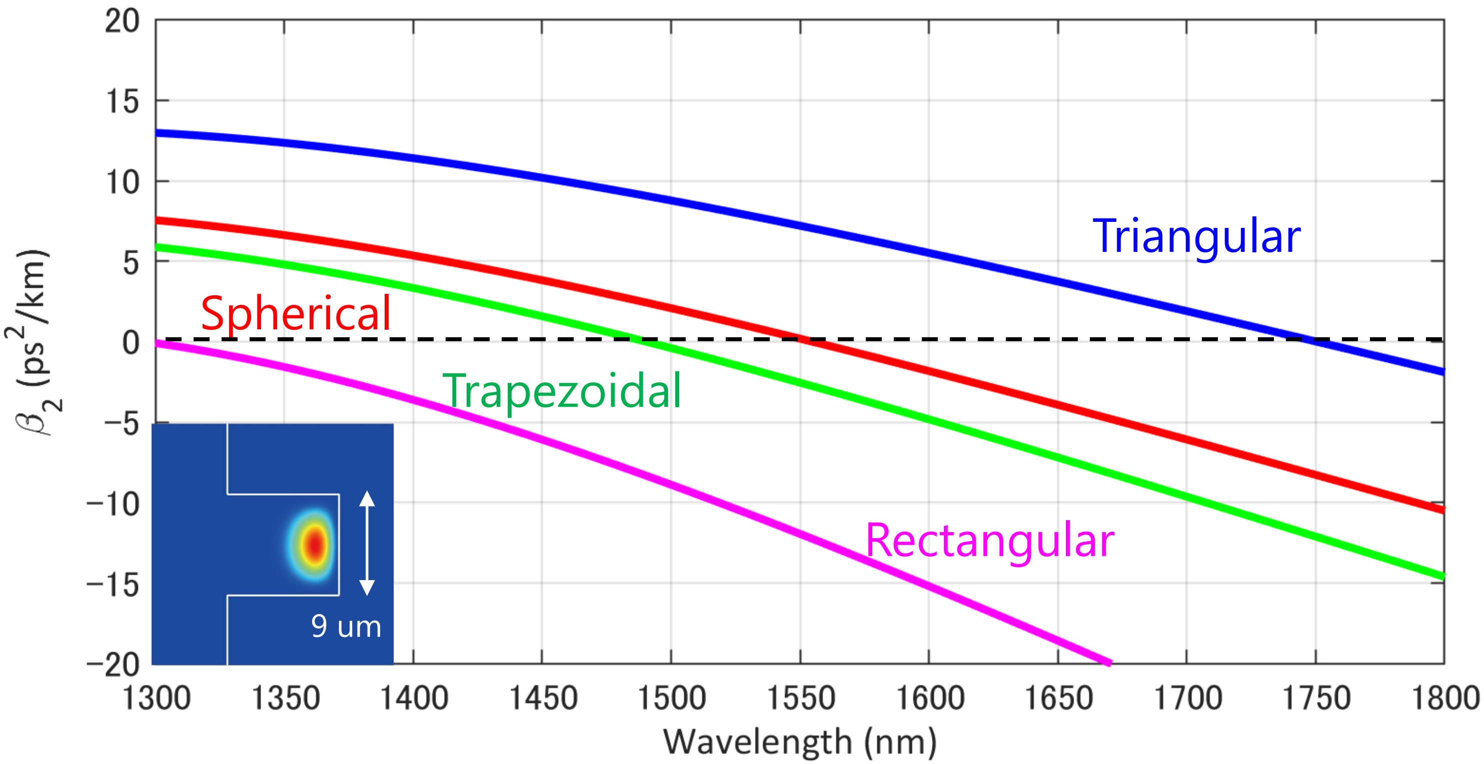

- Degree of freedom of structures allows us to control resonator dispersion
- Rectangular shape is ideal for realizing anomalous group-velocity dispersion

Machining of single crystal materials

Crystallographic image of CaF_2 material

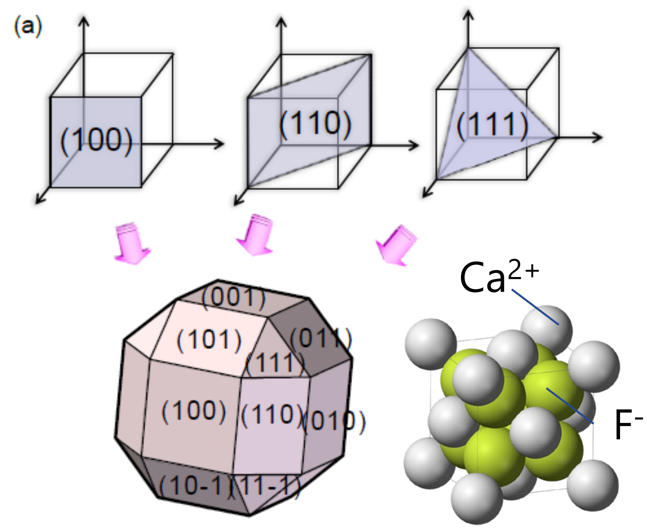

- Plane of single crystal is defined as mirror index
- CaF_2 consists of only 3 planes (100), (110), (111)
- Cutting mode transition observed with cutting depth

Slip formation (100)[110]

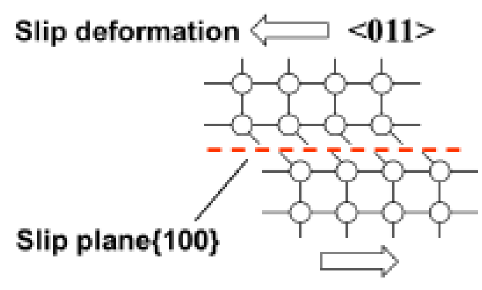

More ductile

Cleavage formation (111)

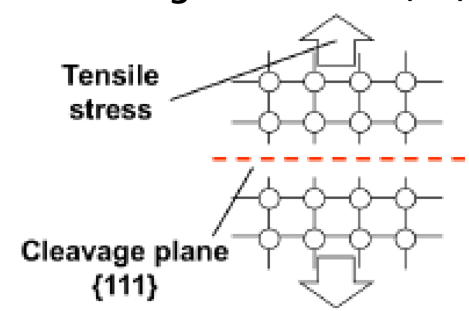

Very brittle

Cutting mode transition is observed depending on crystal anisotropy

Ductile-mode cutting

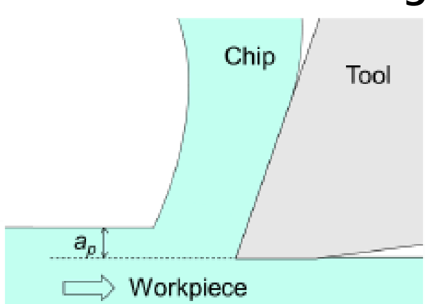

Cutting depth < Critical depth

Brittle-mode cutting

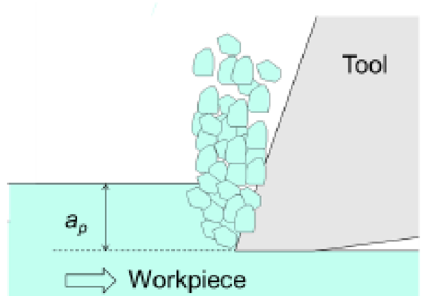

Cutting depth > Critical depth

Transition to brittle mode as cutting material

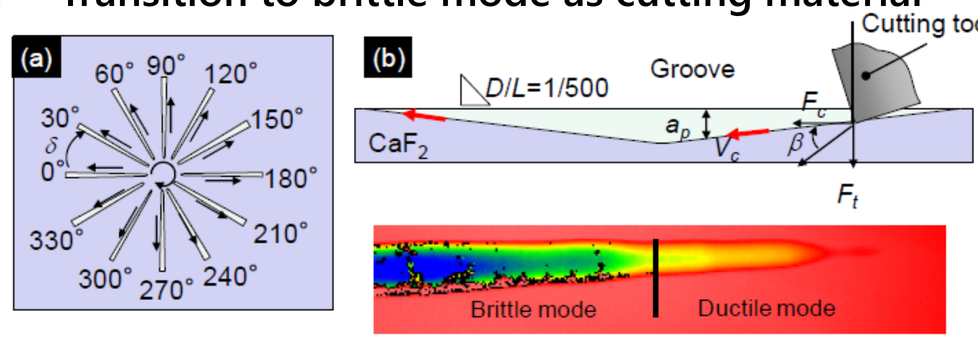

Precision Engineering 40 (2015) 172–181

Cylindrical turning experiment

Experimental setup

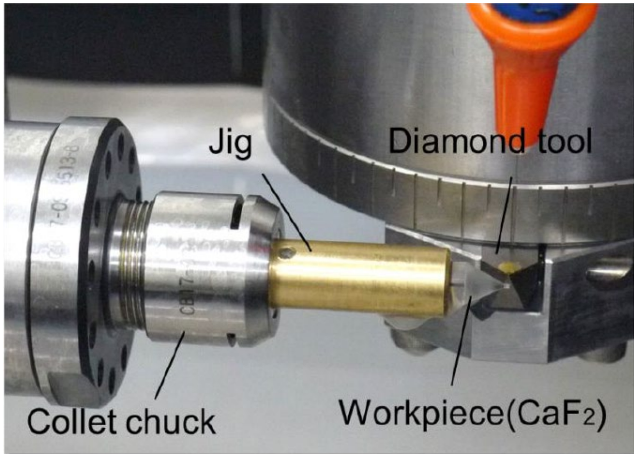

"Objective" of cylindrical turning experiment

- Cutting plane and direction are continuously and simultaneously changed when resonator is turned
- Investigate surface roughness of entire cylindrical surface

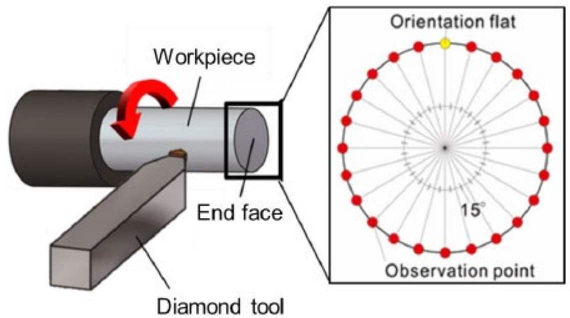

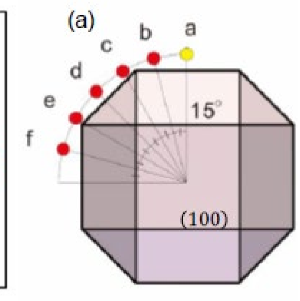

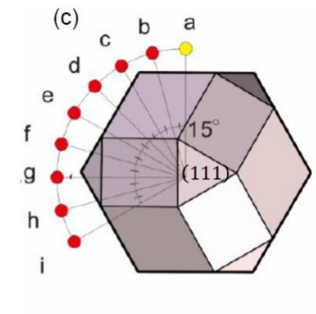

Cylindrical surface roughness for observation points with different end-faces

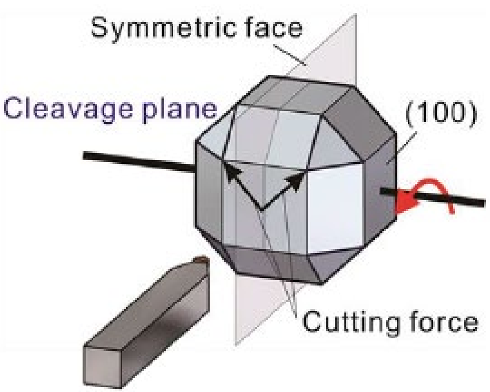

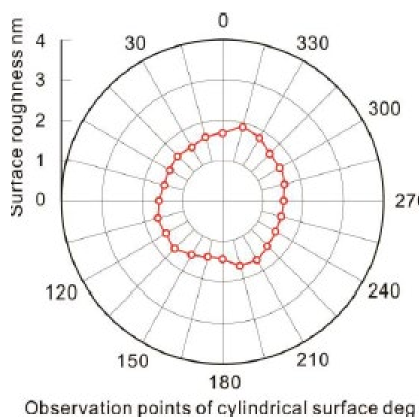

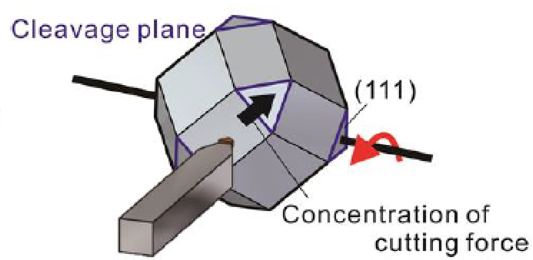

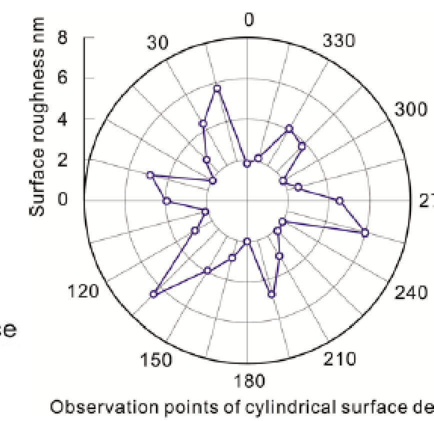

Observed smooth surface with end-face (100)

Observed surface clack with the end-face (111)

Precision Engineering 40 (2015) 172–181   Precision Engineering 49 (2017) 104–114

Ultra-precision machining procedure

Experimental setup and machine used

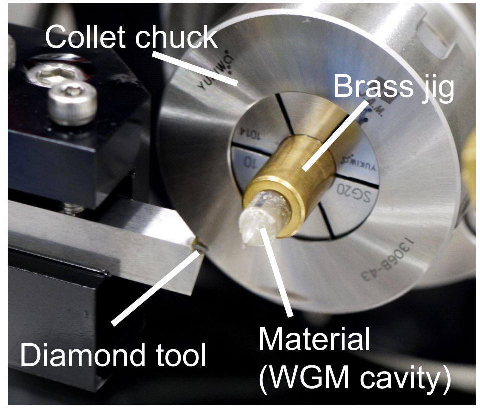

Manufacturing parameters

- Rotation speed [min^{-1}]
- Cutting speed [m/min]
- Feed per revolution [um/rev]
- Depth of cut [nm]
- End-face orientation
- Lubricant
- Nose radius (cutting tool)
- Rake angle (cutting tool)

Fabrication flow of ultra-precision turning for *triangular* cross-section microresonator

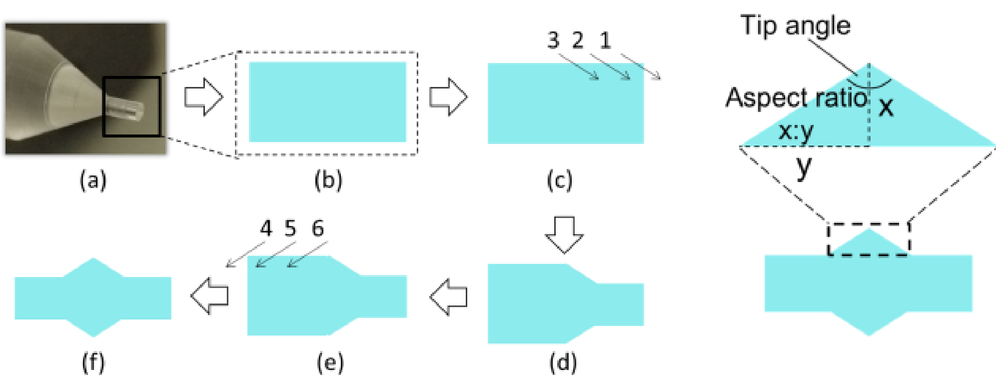

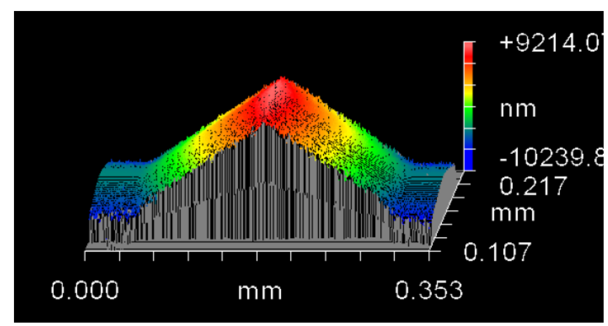

- The tip angle and the aspect ratio are pre-designed and formed by computer-controlled turning, which is attractive with respect to dispersion engineering

Experimental setup

Experimental setup for Q-factor and dispersion measurement

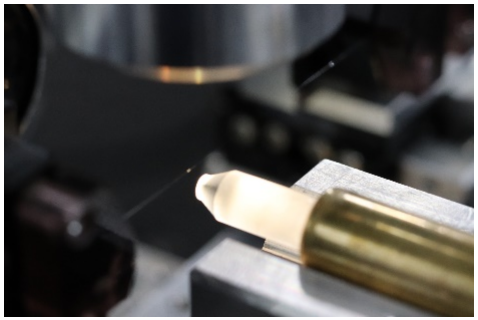

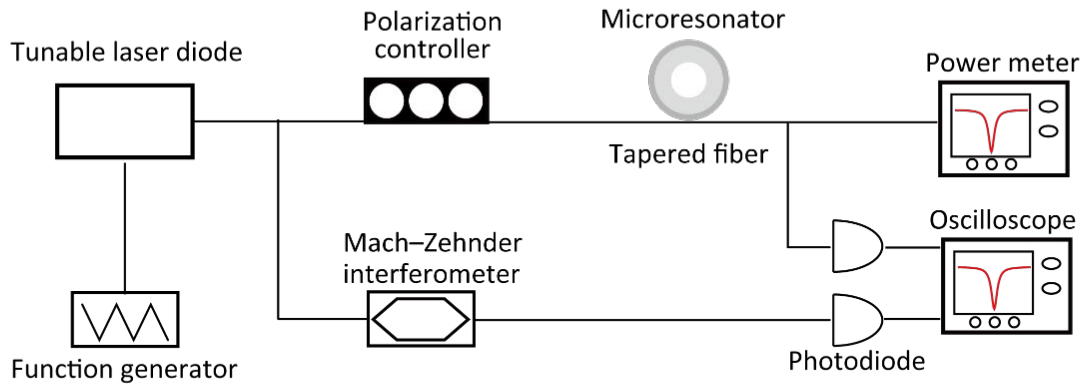

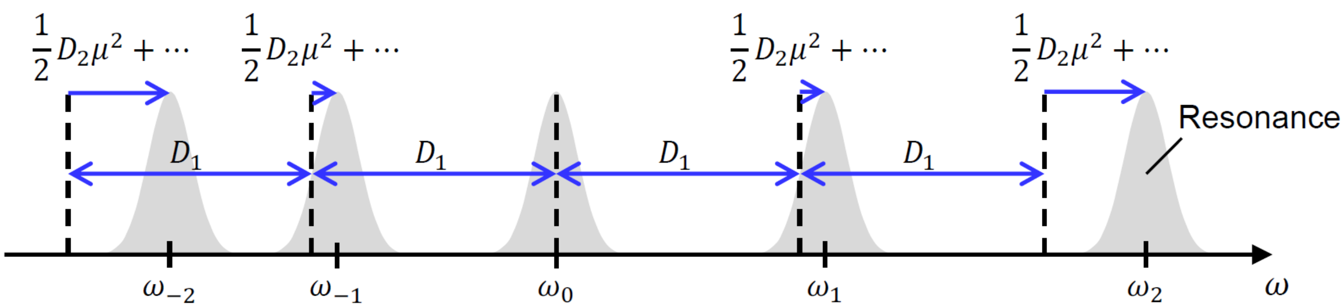

Group-velocity dispersion

$D_2 > 0$: anomalous
$D_2 < 0$: normal

Resonance frequency: $\omega_m = \frac{2\pi mc}{Ln(\omega)}$

Resonance frequencies are Taylor-expanded:

$$\omega_\mu = \omega_0 + D_1\mu + \frac{1}{2}D_2\mu^2 + \frac{1}{6}D_3\mu^3 + \cdots$$

m: mode number
μ: mode number offset (from pump $\mu = 0$)

Mach-Zehnder interferometer calibrates frequency axis

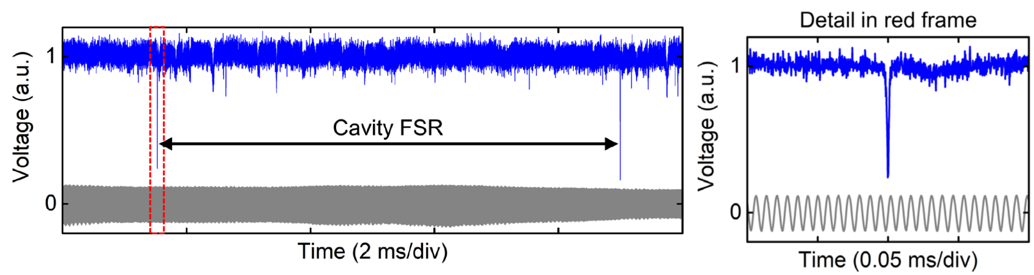

Measured Q-factor and dispersion

Crystalline microresonator fabricated *"without polishing"*

Spherical MgF_2 WGM Diameter 508 μm Curvature 36 μm

paper in preparation

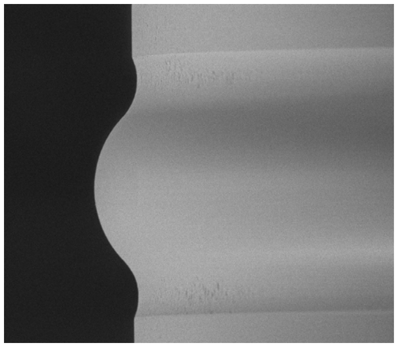

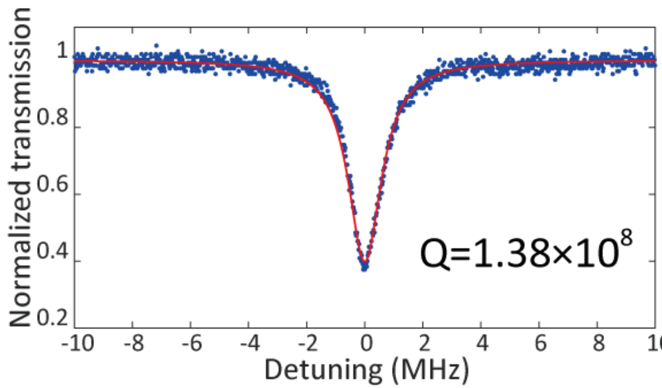

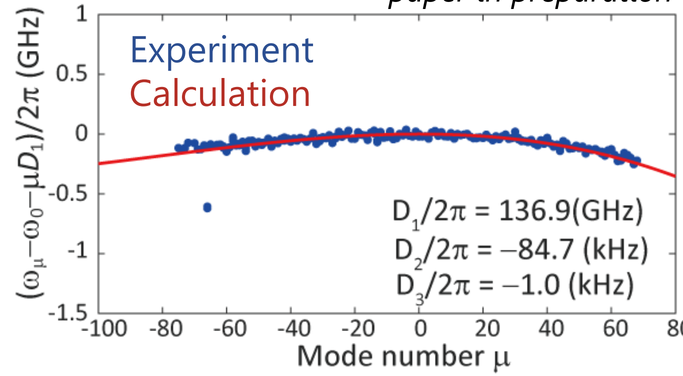

Triangular CaF_2 WGM Diameter 502 μm Apex angle 120°

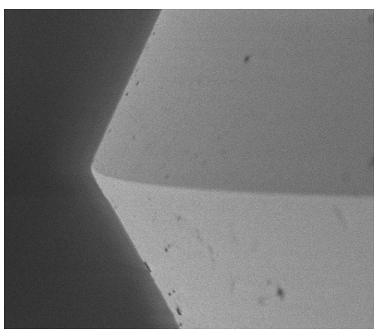

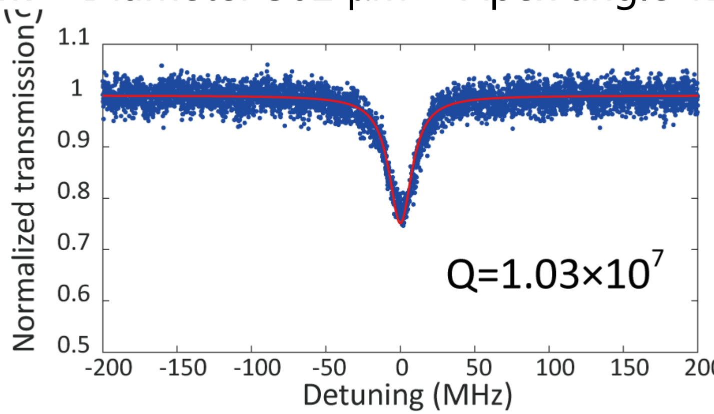

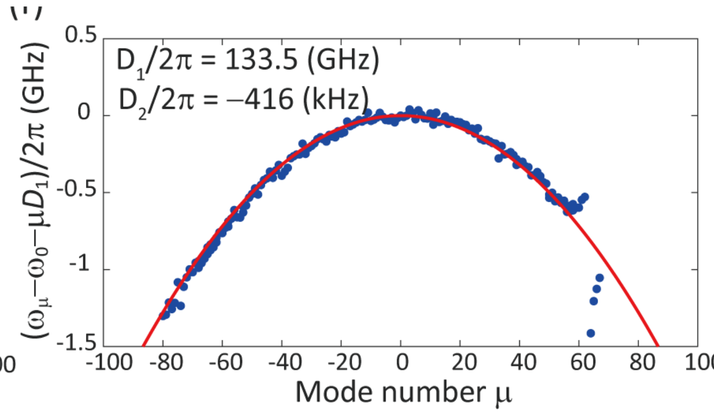

- Highest Q-factor exceeding 10^8 was observed in MgF_2 spherical WGM resonator
- Effect of crystal anisotropy and best end-face should be investigated
- MgF_2 is more suitable for Kerr comb generation as regards thermal stability

Octave-wide phase-matched FWM

- Numerical simulation (LLE)

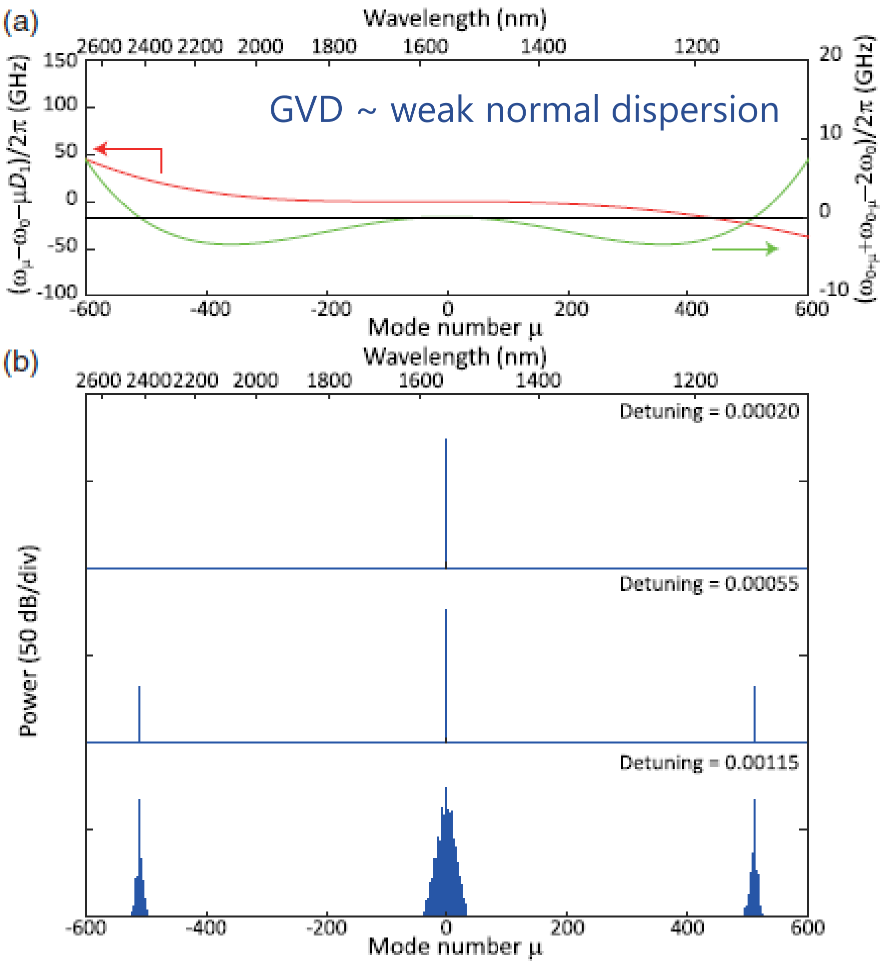

- Experimental observation

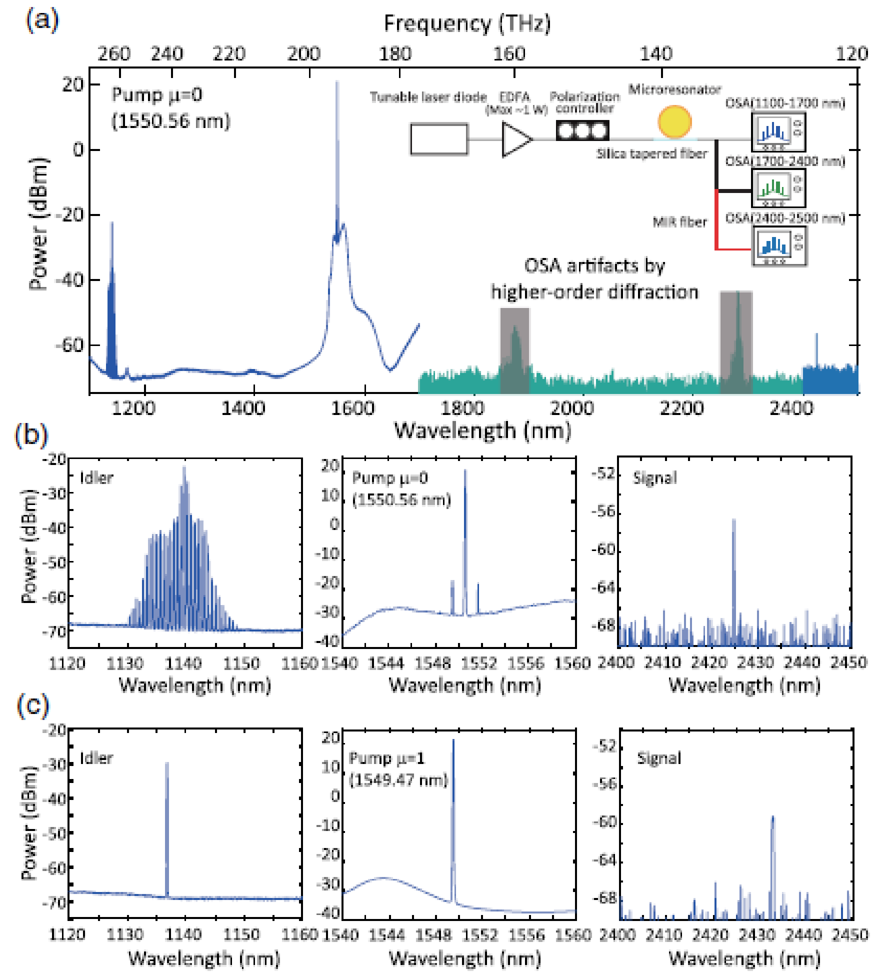

S. Fujii et al., Optics Letters 44, 3146 (2019).

- FWM sidebands spanning one-octave via higher-order dispersion (4th order dispersion)
- Numerical simulation agrees well with experimental observation

Conclusion

- Proposed ideal WGM structure for 100-GHz FSR microcomb in MgF_2 crystalline microresonators (rectangular shapes achieve anomalous dispersion in 1550 nm)
- Identified critical depth and for each end-face orientation to acheive ultra-precision machining of crystalline microresonators
- Observed highest Q exceeding 10^8 and microcomb without polishing process
- Demonstrated octave-wide FWM in dispersion-engineered microresonators

Thank you

Publication

S. Fujii et al., "Octave-wide phase-matched four-wave mixing in dispersion engineered crystalline microresonators", Optics Letters **44**, 3146 (2019).

Acknowledgment

This work is supported by Japan Society for the Promotion of Science (JSPS) KAKENHI under Grant Number JP19H00873, JP18J21797 and Grant-in-Aid for JSPS Fellow; Amada Foundation; The Ministry of Education, Culture, Sports, Science and Technology (MEXT) Q-LEAP, and SCOPE 191603001 from MIC.

We thank Dr. Y. Mizumoto, H. Kangawa for their contribution of this work